Available online at www.sciencedirect.com

ScienceDirect

Energy Procedia 158 (2019) 5557–5562

Energy Procedia

www.elsevier.com/locate/procedia

10th International Conference on Applied Energy (ICAE2018), 22-25 August 2018, Hong Kong, China

# Research on Quantitative Relationship between Fire Separations and Ampacity in Underground pipe gallery Electric cabin

Jiaxu WANG[a], Xuefeng LIU[a,*], Shu LI[a] ,Guanyu Fang[b], Wenjing Chen[b], Shiming Deng[b]

[a]South China University of Technology, School of Electric Power , Wushan RD., Tianhe District, Guangzhou, 510641, P.R. China
[b]The Hong Kong Polytechnic University, Department of Building Services Engineering, Hung Hom, Kowloon, Hong Kong, 999077

**Abstract**

In recent years, underground pipe gallery has become more and more important. Its Special working environment makes temperature monitoring and control increasingly important. paper applies heat-transfer differential equation to the cable to obtain the similarity criterion of cable temperature distribution. After calculating the electric cabin model with different fire separations, it is found that the temperature distribution of the same ampacity in different fire separations conforms to certain rules. The temperature distribution of different ampacity in the same fire separation is also regular: the ampacity rises. 5%, temperature rises by 7%. As a result, the fitting formulas of the current carrying capacity, the length of the fire separation and the location of the highest temperature were also proposed.



*Keywords:* Underground pipe gallery; similarity criterion; dimensionless number; fire separation; cable ampacity

**Nomenclature**

| | |
|---|---|
| T | temperature |
| $T_\infty$ | Inlet air temperature |

* Corresponding author. Tel.: +86 13580456068.
*E-mail address:* lyxfliu@scut.edu.cn


10.1016/j.egypro.2019.01.587

| | |
|---|---|
| r | Point to cable core axis distance |
| λ | thermal conductivity |
| $\dot{\Phi}$ | heat source density |
| θ | cable core dimensionless temperature( $\theta = T/T_\infty$) |
| Θ | cable insulator( $\Theta = (T-T_\infty)/T_\infty$) |

## 1. Introduction

Underground pipe gallery can effectively solve the problems of land resources lackness, unreasonable pipelines laying etc. It can efficiently use urban underground space to make the city beautiful. Therefore, the construction of an underground pipe gallery will become more common in the future.

The large construction volume of underground pipe projects makes it difficult to predict operating conditions in advance and lacks technical standards. The scale model that can be verified by experiments has become an effective way to simulate the temperature distribution of the electric cabin and to study the heat transfer characteristics of the electric cabin cable[1-3]. At present, the finite element simulation software is used at domestic and foreign to calculate the cable temperature distribution[2-5]. For the experimental calculation of cable core temperature, predicted the ampacity of power cables by measuring the sheath temperature of cable insulation is Acceptable[3-5]. Several studies have also been conducted on cable temperature in different environments, [6]studied the difference in the temperature of power cables under different environments such as the cable spacing and the cable layer. Further, the effect of pitch and cable trench depth on cable temperature was also studied[7-10]. [6]. In some articles, the effects of ambient conditions such as cyclical changes in the surface temperature and the continuous operation of the cable over a period of time are taken into consideration[11-13].

In this paper, the temperature field is simplified to a one-dimensional model, and the Dimensionless number of the cable temperature in the electric cabin is proposed from the differential equation of heat transfer. By numerically efficient simulation tool, the relationship between fire separation and ampacity was studied. The law of cable temperature distribution and the fitting formula were obtained through the experiment in order to make the future more convenient to study the heat transfer of the cable.

## 2. Physical model of temperature field in electric cabin

### *2.1. Cable core temperature field model*

Due to the long cable span, less bending, and large shaft diameter ratio, the experiment ignored the radial heat conduction of the cable core. To make equation Dimensionless, Defining $\theta = T/T_\infty$. Therefore, one-dimensional cable core temperature field function can be obtained based on the Fourier heat conduction equation:

$$\theta = f(x, \dot{\Phi} r r_1 / 2\lambda_1 T_\infty) \tag{1}$$

Therefore $\dot{\Phi} r^2_1 / 2\lambda_1 T_\infty$ is a Dimensionless number.

### *2.2. Cable insulation temperature field model*

Convective heat transfer is the mainly. boundary condition of insulation. Defining $T - T_w = \phi$; $(T - T_w)/T_\infty = \Theta$ to make equation Dimensionless:

$$\Theta = f\left(\frac{r}{r_2}; \frac{\dot{\Phi} r_1 r_2}{2\lambda_2 T_\infty}; \frac{h r_2}{\lambda_2}\right) \tag{2}$$

It can be seen from the above formula that $\dot{\Phi} r_1 r_2 / 2\lambda_2 T_\infty$ and $hr_2 / \lambda_2$ are Dimensionless number which determine the temperature field of cable core.

## 3. Method and procedure

### *3.1. model*

In order to verify the reliability of similar theory, this paper sets up two models: model1, model2. The parameter provided by the relevant units is shown in the table1:

Table 1. Cable parameters

| Parameters | Value | Parameters | Value |
|---|---|---|---|
| Electric cabin cross-sectional area ($m^2$) | 9 | Cable core resistivity | 0.00000002 |
| Cable diameter (m) | 0.25 | Thermal conductivity of air (w/(m • k)) | 0.0243 |
| Voltage (kV) | 220 | Thermal conductivity of wall (w/(m • k)) | 1.74 |
| Ampacity (A) | 1900 | Thermal conductivity of solid (w/(m • k)) | 1 |
| Number of cable cores | 1 | Thermal conductivity of insulator (w/(m • k)) | 0.3 |
| Cable core cross-sectional area ($m^2$) | 0.0075 | Thermal conductivity of cable core (w/(m • k)) | 401 |

The calculation formula for the heat value per meter of a single cable core provided by the relevant unit is $Q = \rho I^2 / S$,( $\rho$ is cable core resistivity; $S$ is cable core cross-sectional area). So the real cable heat value per meter is 346.6w/m. Model 2 is a laboratory test bench model, which uses electric heaters to simulate heat source and lagging to simulate insulator. According to Dimensionless number $\dot{\Phi} r_1 r_2 / 2\lambda_2 T_\infty$, heat value per meter of model1 is 61.96w/m and model2 is 7.8w/m. The model parameters are shown in the table2:

Table 2. Model parameters

| Model Parameters | Value |
|---|---|
| Insulator Inner radius of model1 (m) | 0.0097 |
| Insulator Outer radius of model1 (m) | 0.025 |
| Heat value of model1 (w/m) | 61.96 |
| Insulator Inner radius of model2 (m) | 0.0065 |
| Insulator Outer radius of model2 (m) | 0.015 |
| Heat value of model2 (w/m) | 7.8 |

### *2.2 Sketch of model*

Front view, and side view of model is shown in Figure1.

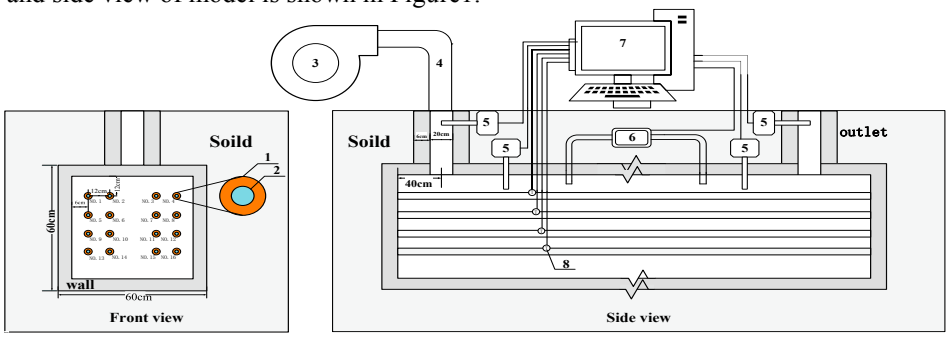

Figure. 1. Front view and side view of model
1—insulation；2—cable core；3—fan；4—wind duct；5—anemometer；6—differential pressure pickup；7—computer；8—thermocouple

The numbers in front view are the serial numbers of the cables. The cables 1, 5, 9 and 13 are defined as the external cables. The 2, 6, 10, 14 cables are inner row cables.

## 5. The relationship of fire separation and cable load

During the construction of the electric cabin, fire separations with vents need to be built. In this paper, several simulation experiments were conducted to explore the relationship between the ampacity and the length of the fire separations. The length of fire separations in the electric cabin for the scale models in the experiment were: 12m, 18m, 24m, 30m, 36m. The corresponding is 60m, 90m, 120m, 150m, 180m. As shown in the previous table, the full load condition has a current carrying capacity of 1900A, a variable load of 90%, and 80% of the ampacity, that is, 1710A and 1520A. Due to limited space, only the calculation results at 12m, 18m, and 24m are shown.

### *5.1. Temperature distribution of external cables in different fire separation at full load*

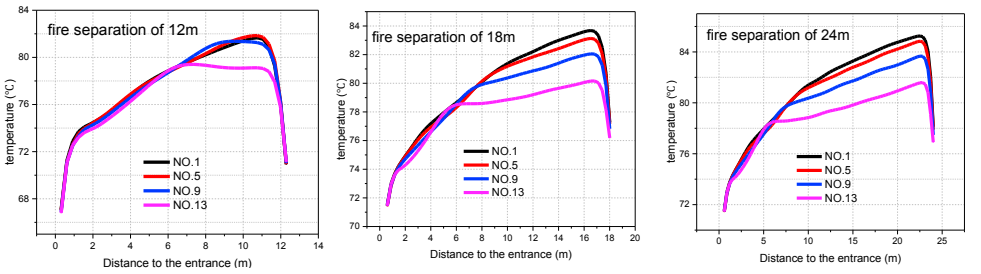


Figure. 2. Temperature distribution of full-load cables at different fire separations

In the first 6 meters, the temperature of each cable in the electric cabin is relatively close, but the temperature difference becomes apparent after 6m. The temperature of No. 1 cable is the highest, and the temperature of No. 13 cable is the lowest. As the distance increases, the temperature of the No. 5 cable will gradually increase and exceed that of the No. 1 cable. At the same time, the temperature is close to the limit temperature of 90° C, therefore the No. 1 cable temperature is still the highest.

### *5.2. Temperature comparison and function fitting of No.1 cable in different fire separation under different loads*

It can be seen that the maximum temperature of No. 1 cable and its position is a logarithmic function when the fire prevention interval is gradually extended. After the fire prevention interval is increased, the computer simulation closely matches the calculated results of the existing length.

The fitting formulas under different loads are as follows:

Table 3. Functional expressions under different loads

| load | Functional expression | A0 | t1 | y0 |
|---|---|---|---|---|
| 100% | $y = A_0 e^{(-x/t_1)} + y_0$ | -15.62716 | 15.15619 | 89.02146 |
| 90% | $y = A_0 e^{(-x/t_1)} + y_0$ | -12.60645 | 15.64293 | 77.85372 |
| 80% | $y = A_0 e^{(-x/t_1)} + y_0$ | -9.63776 , | 14.2057 | 67.3201 |

## 5 Prediction and verification of fitting formulas

Parameters of fitting formulas obtained in Figure 3 are constantly changing under different load. Organize the parameters into a graph:

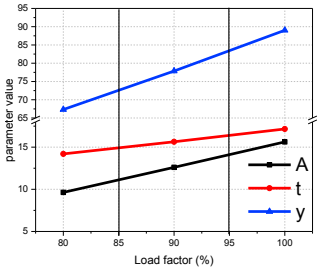


Figure. 3. Fitting formula parameters and load rate diagram

It can be seen that A1, t1, y0 are distributed linearly with the load rate, and they satisfy: $A_0 = -0.29947x + 14.31984$; $t_1 = 0.1425x + 2.8057$; $y_0 = 1.085x - 19.4799$. Then A1, t1, and y0 at 85% load are:-11.13511; 14.8192; 72.7454. and A1, t1, y0 at 95% load are: -14.12981; 16.3432; 83.5951.

The temperature curve of No. 1 cable under different fireproof intervals at 85% and 95% load and the function fitting curves are shown in the figure 4:

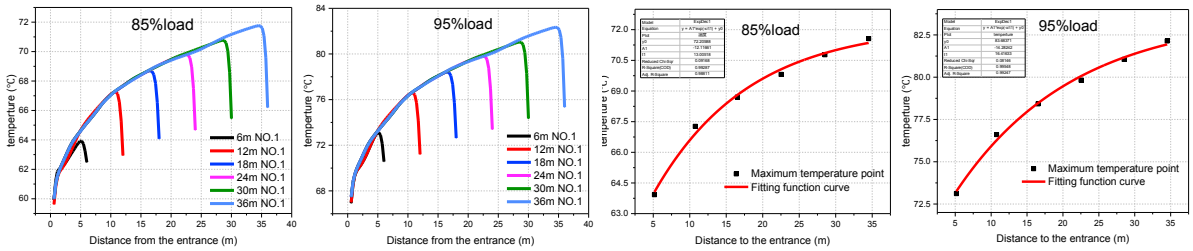


Figure. 4. Maximum temperature point for 85% and 95% load cables at different fire separation and Fitting functions

From fig.5, it can be seen that A1, t1, and y0 at 85% load are: −111.661242; 14.43356; 72.45786, the A1, t1, and y0 at 95% load are −14.19997; 15.97402; 83.51166, respectively. The specific results obtained and numerical predictions can be derived from the table 5:

Table 4. Calculation and verification of fitting formula parameters

| Parameters | Predictive value at 85% load | Function fitting value at 85% load | Percent difference | Predictive value at 95% load | Function fitting value at 95% load | Percent difference |
|---|---|---|---|---|---|---|
| A1 | -11.13511 | -11.61242 | 4.29% | -14.12981 | -14.19997 | 0.49% |
| t1 | 14.9182 | 14.43356 | 3.25% | 16.3432 | 15.9740 | 2.31% |
| y0 | 72.7454 | 72.45786 | 0.39% | 83.5951 | 83.51166 | 0.1% |

The difference between the theoretical formula's fitting formula parameters and the simulation calculation is less than 5%, which is reliable. The relationship between the location of the highest temperature point of the different load cables and the length of the fire separation can be expressed by the following formula:

$$y = (-0.29947w + 14.31984)\,e^{\left[-x/(0.1425\left(\frac{w}{1900}\right)+2.8057)\right]} + (1.085w - 19.4799) \tag{3}$$

Where y is temperature of cable core; x is measuring point to air inlet distance; w is cable ampacity.

## 6. Conclusions

- When changing the cable ampacity, the cable temperature moves up and down compared to the standard operating conditions, verifying the similarity theory obtained above.
- In the same load conditions, the maximum temperature of the cable has a significant relationship with the fire separation, which is approximately a logarithmic curve.
- The relationship between the location of the highest temperature point of the different load cables and the length of the fire separation are obtained.

## 7. Discussion

The experimental verification will be carried out in the follow-up work. The construction method of the experimental platform has been given in Figure 1, and it has been completed. The effect of localized intense turbulence at the fire-fighting interval on the air inlet and outlet and the quantified relationship will be demonstrated in future work, and the impact of radiation will also be taken into consideration.

## Acknowledgment

This study is supported by the National Natural Science Foundation of China (Grant No. 51778234), the Natural Science Foundation of Guangdong Province (Grant No. 2015A030310303), Guangdong Provincial Science, Technology Project (Grant No. 2017A020216024) and Special Funds for Basic Scientific Research Business Fees for Central Universities (Grant No. B6150170) and Guangdong Province Key Laboratory of Efficient and Clean Energy Utilization

## Reference

[1] Mingxiang Wu, Xianbo Deng, Songhua Liu. Calculation of Temperature Field Distribution and Current Carrying Capacity of Cable in Typical Laying Mode[J]. Hubei Electric Power, 2012, 36(6):37-39.

[2] Adefarati T, Bansal R C. Integration of renewable distributed generators into the distribution system: a review[J]. Iet Renewable Power Generation, 2016, 10(7):873-884.

[3] Xiaoliang Zhuang. Distribution Cable Operation Monitoring and Current Carrying Capacity Prediction Based on Fiber Temperature Measurement Based on Fiber Temperature Measurement [D]. South China University of Technology,2015.

[4] Boukrouche F, Moreau C, Pelle J, et al. Mock-up Study of the Effect of Wall distance on the Thermal Rating of Power Cables in Ventilated Tunnels[J]. IEEE Transactions on Power Delivery, 2016, PP(99):1-1.

[5] Yongming Yang, Peng Cheng, Jun Chen. Research on Cable Heat Dissipation Considering Effect of Air Flow Field and Its Influence Factors and Economic Analysis [J]. Electric Power Automation Equipment, 2013, 33(1):50-54.

[6] Boukrouche F, Moreau C, Pelle J, et al. Mock-up Study of the Effect of Wall distance on the Thermal Rating of Power Cables in Ventilated Tunnels[J]. IEEE Transactions on Power Delivery, 2016, PP(99):1-1.

[7] Wędzik A, Siewierski T, Szypowski M. A new method for simultaneous optimizing of wind farm's network layout and cable cross-sections by MILP optimization[J]. Applied Energy, 2016, 182:525-538.

[8] Cheung H, Wang S, Zhuang C, et al. A Simplified Power Consumption Model of Information Technology (IT) Equipment in Data Centers for Energy System Real-time Dynamic Simulation[J]. Applied Energy, 2018, 222.

[9] Baldinelli G, Bianchi F. Windows thermal resistance: Infrared thermography aided comparative analysis among finite volumes simulations and experimental methods[J]. Applied Energy, 2014, 136(136):250-258.

[10] Lee H, Sharp J, Stokes D, et al. Modeling and analysis of the effect of thermal losses on thermoelectric generator performance using effective properties[J]. Applied Energy, 2018, 211:987-996.

[11] Vrana T K, Mo O. Optimal Operation Voltage for Maximal Power Transfer Capability on Very Long HVAC Cables ☆[J]. Energy Procedia, 2016, 94:399-408.

[12] Wan I W M N, Royapoor M, Wang Y, et al. Office building cooling load reduction using thermal analysis method – A case study[J]. Applied Energy, 2017, 185:1574-1584.

[13] Reddy B S, Chatterjee D. Analysis of High Temperature Low Sag Conductors Used for High Voltage Transmission ☆[J]. Energy Procedia, 2016, 90:179-184.